

## Measuring a Parity-Violation Signature in the Early Universe via Ground-Based Laser Interferometers

Naoki Seto<sup>1,2</sup> and Atsushi Taruya<sup>3</sup>

<sup>1</sup>*National Astronomical Observatory, 2-21-1 Osawa, Mitaka, Tokyo 181-8588, Japan*

<sup>2</sup>*Department of Physics and Astronomy, 4186 Frederick Reines Hall, University of California, Irvine, California 92697, USA*

<sup>3</sup>*Research Center for the Early Universe, School of Science, University of Tokyo, Tokyo 113-0033, Japan*

(Received 28 March 2007; published 17 September 2007)

We show that pairs of widely separated interferometers are advantageous for measuring the Stokes parameter  $V$  of a stochastic background of gravitational waves. This parameter characterizes asymmetry of amplitudes of right- and left-handed waves, and generation of the asymmetry is closely related to parity violation in the early universe. The advantageous pairs include the kilometer-size interferometers LIGO (Livingston)-LCGT and AIGO-Virgo, which are relatively insensitive to  $\Omega_{\text{GW}}$  (the simple intensity of the background). Using at least three detectors, information of the intensity  $\Omega_{\text{GW}}$  and the degree of asymmetry  $V$  can be separately measured.

DOI: 10.1103/PhysRevLett.99.121101

PACS numbers: 95.55.Ym, 95.85.Sz, 98.80.Es

*Introduction.*—Stochastic background of gravitational waves is one of the most important targets for gravitational-wave astronomy [1]. Because of the weakness of gravitational interaction, our universe is transparent to the background up to very early epochs, and we might uncover interesting nature of the universe at extremely high-energy scales, through observational studies of the stochastic background. To extract the information as much as possible, we need to characterize the background efficiently in a model independent manner, and investigation beyond simple spectral analysis might yield a great discovery. In this respect, circular polarization degree, which describes the asymmetry between the amplitudes of right- and left-handed waves, may be a fundamental characteristic of the background to probe the early universe. Because the parity transformation relates these two polarization modes, the asymmetry in the stochastic gravitational waves directly reflects a parity violation in the early universe, for instance, generated through the gravitational Chern-Simons term (e.g., [2]). Since the observed universe is highly isotropic and homogeneous, we shall focus on the monopole component of the circular polarization as our primary target and report principle aspects for its measurement with a network of ground-based interferometers (see [3,4]).

*Circular polarization.*—Let us first describe circular polarization of a gravitational-wave background. We use a plane wave expansion of the background as [5,6]

$$h_{ij}(t, \mathbf{x}) = \sum_{P=+, \times} \int_{-\infty}^{\infty} df \int_{S^2} d\mathbf{n} h_P(f, \mathbf{n}) e^{2\pi i f(-t + \mathbf{n} \cdot \mathbf{x})} e_{ij}^P(\mathbf{n}). \quad (1)$$

Here, the amplitude  $h_P$  is the mode coefficient that is a stochastic and random variable. The bases for transverse-traceless tensor  $e^P$  ( $P = +, \times$ ) are given as  $e^+ = \hat{e}_\theta \otimes \hat{e}_\theta - \hat{e}_\phi \otimes \hat{e}_\phi$  and  $e^\times = \hat{e}_\theta \otimes \hat{e}_\phi + \hat{e}_\phi \otimes \hat{e}_\theta$ , with unit vectors  $\hat{e}_\theta$  and  $\hat{e}_\phi$ . These vectors are normal to the propagation

direction  $\mathbf{n}$ , associated with a right-handed Cartesian coordinate as usual. As an alternative characterization, we can use the circular polarization bases  $e^R = (e^+ + ie^\times)/\sqrt{2}$  (right-handed mode) and  $e^L = (e^+ - ie^\times)/\sqrt{2}$  (left-handed mode) for the plane wave expansion (1). The corresponding amplitudes  $h_R$  and  $h_L$  are given by  $h_R = (h_+ - ih_\times)/\sqrt{2}$  and  $h_L = (h_+ + ih_\times)/\sqrt{2}$ . The ensemble average of their amplitudes is classified as

$$\left( \begin{array}{c} \langle h_R(f, \mathbf{n}) h_R(f', \mathbf{n}')^* \rangle \\ \langle h_L(f, \mathbf{n}) h_L(f', \mathbf{n}')^* \rangle \end{array} \right) = \frac{\delta_{\mathbf{n}, \mathbf{n}'} \delta_{f, f'}}{4\pi} \left( \begin{array}{c} I(f, \mathbf{n}) + V(f, \mathbf{n}) \\ I(f, \mathbf{n}) - V(f, \mathbf{n}) \end{array} \right), \quad (2)$$

with the functions  $\delta_{Y,Z}$  being delta functions. In the above expression, the real function  $V$  characterizes the asymmetry between the amplitudes of the right- and left-handed waves, while the function  $I$  ( $\geq |V|$ ) represents their total amplitude. Note that the other combinations, such as  $\langle h_R h_L^* \rangle$  and  $\langle h_L h_R^* \rangle$ , describe the linear polarization mode and are proportional to  $Q \pm iU$ , combinations of two other Stokes parameters. In this Letter, we do not study the linear polarization  $Q \pm iU$ , since they do not have an isotropic component. We will focus on the detectability of the isotropic components  $I(f)$  and  $V(f)$ . Using the normalized logarithmic energy density of the background  $\Omega_{\text{GW}}(f)$  [5,6], the two functions  $I$  and  $V$  are expressed as

$$I(f) = \frac{\rho_c}{4\pi f^3} \Omega_{\text{GW}}(f), \quad V(f) = \frac{\rho_c}{4\pi f^3} \Omega_{\text{GW}}(f) \Pi(f), \quad (3)$$

where  $\rho_c$  is the critical density of the Universe,  $\rho_c = 3H_0^2/8\pi$ , with  $H_0 = 70h_{70} \text{ km sec}^{-1} \text{ Mpc}^{-1}$  being the Hubble parameter. The ratio  $\Pi(f) = V(f)/I(f)$  characterizes the circular polarization degree. For simplicity, we assume the flat spectra,  $\Omega_{\text{GW}}(f) \propto f^0$  and  $\Pi(f) \propto f^0$ , as our fiducial model. Thus, our main interest is the simultaneous measurements of the parameters  $\Omega_{\text{GW}}$  and  $\Pi$ .

We next consider how to detect the isotropic components of  $I$  and  $V$  modes with laser interferometers such as the LIGO. Let us recall that the output signal  $s_a$  of a detector  $a$  at the position  $\mathbf{x}_a$  is written as  $s_a(f) = \sum_{P=+, \times} \int_{S^2} d\mathbf{n} h_P(f, \mathbf{n}) F_a^P(\mathbf{n}, f) e^{i2\pi f \mathbf{n} \cdot \mathbf{x}_a}$ . Here, the function  $F_a^P$  is the beam pattern function and it represents the response of the detector to a polarization mode  $e^P$ . Provided the data streams  $s_a$  and  $s_b$  taken from two detectors  $a$  and  $b$ , the detection of stochastic signals can be achieved by taking a cross-correlation,  $\langle s_a(f) s_b(f')^* \rangle \equiv C_{ab}(f) \delta_{f, f'}$ . Keeping the signals from the isotropic components, the correlation signal  $C_{ab}(f)$  is written as

$$C_{ab}(f) = \gamma_{I,ab}(f) I(f) + \gamma_{V,ab}(f) V(f), \quad (4)$$

where the quantity  $\gamma_I$  is the overlap function given by [5,6]

$$\gamma_{I,ab}(f) = \frac{5}{8\pi} \int_{S^2} d\mathbf{n} [\{F_a^+ F_b^{+*} + F_a^\times F_b^{\times*}\} e^{i\mathbf{y} \cdot \mathbf{n} \cdot \mathbf{m}}], \quad (5)$$

with  $\mathbf{y} \equiv 2\pi f D/c$ . Here, we have expressed  $\mathbf{x}_a - \mathbf{x}_b$  as  $D\mathbf{m}$  ( $D$  is the distance;  $\mathbf{m}$  is a unit vector). Similarly, the function  $\gamma_{V,ab}(f)$  is obtained by replacing the kernel  $[\cdot \cdot \cdot]$  in Eq. (5) with  $[i\{F_a^+ F_b^{\times*} - F_a^\times F_b^{+*}\} e^{i\mathbf{y} \cdot \mathbf{n} \cdot \mathbf{m}}]$ .

*Overlap functions for ground-based detectors.*—Now, specifically consider the response of an L-shaped interferometer  $a$  on the Earth. We assume that the detector has two orthogonal arms with equal arm length. Denoting the unit vectors parallel to the two arms by  $\mathbf{u}$  and  $\mathbf{v}$ , the beam pattern function takes a simple form as  $F_a^P = \mathbf{d}_a \cdot \mathbf{e}^P(\mathbf{n})$ , with  $\mathbf{d}_a = (\mathbf{u} \otimes \mathbf{u} - \mathbf{v} \otimes \mathbf{v})/2$ , where the colon represents a double contraction. This expression is always valid as long as the wavelength of the gravitational waves for our interest is much longer than the arm length of the detectors. In this Letter we study the following five ongoing (and planned) kilometer-size interferometers as concrete examples: the Australian International Gravitational Observatory (AIGO, A), the Large-Scale Cryogenic Gravitational Wave Telescope (LCGT, C), LIGO-Hanford (H), LIGO-Livingston (L) and Virgo (V) [7]. Hereafter, we mainly use their abbreviations (A, C, H, L, V).

For the isotropic component of the stochastic background, only the relative configuration of two detectors is relevant with the correlation signal  $C_{ab}$  and we do not care about the overall rotation. Hence, the sensitivity of each pair of detectors to the stochastic background can be characterized by the three angular parameters  $(\beta, \sigma_1, \sigma_2)$  explained in Fig. 1. Their distance is given by  $D = 2R_E \sin(\beta/2)$  ( $R_E = 6400$  km, the radius of the Earth), which determines a characteristic frequency  $f_D \equiv c/(2\pi D)$  for the overlap functions. Following Ref. [5], we define the angles

$$\Delta \equiv (\sigma_1 + \sigma_2)/2, \quad \delta \equiv (\sigma_1 - \sigma_2)/2. \quad (6)$$

The geometrical information about pairs of detectors among the five interferometers is presented in Table I.

In the expression (5), the angular integral can be performed analytically with explicit forms of the pattern

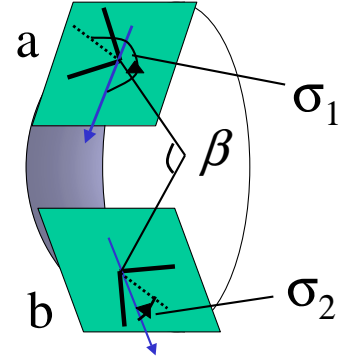


FIG. 1 (color online). Geometrical configuration of ground-based detectors  $a$  and  $b$  for the cross-correlation analysis. Detector planes are tangential to the Earth. The detectors  $a$  and  $b$  are separated by the angle  $\beta$  measured from the center of the Earth. The angles  $\sigma_1$  and  $\sigma_2$  describe the orientation of bisectors of interferometers in a counterclockwise manner relative to the great circle joining two sites.

functions. A long calculation leads to [5]

$$\gamma_{I,ab} = \Theta_1(y, \beta) \cos(4\delta) + \Theta_2(y, \beta) \cos(4\Delta), \quad (7)$$

with  $\Theta_1(y, \beta) = \cos^4(\beta/2)(j_0 + \frac{5}{7}j_2 + \frac{3}{112}j_4)$ , and  $\Theta_2(y, \beta) = (-\frac{3}{8}j_0 + \frac{45}{56}j_2 - \frac{169}{896}j_4) + (\frac{1}{2}j_0 - \frac{5}{7}j_2 - \frac{27}{224}j_4)\cos\beta + (-\frac{1}{8}j_0 - \frac{5}{56}j_2 - \frac{3}{896}j_4)\cos(2\beta)$ . The function  $j_n$  is the  $n$ -th spherical Bessel function with its argument  $y = f/f_D$ .

On the other hand, the overlap function for the  $V$  mode is given by

$$\gamma_{V,ab} = \Theta_3(y, \beta) \sin(4\Delta), \quad (8)$$

with  $\Theta_3(y, \beta) = -\sin(\beta/2)[(-j_1 + \frac{7}{8}j_3) + (j_1 + \frac{3}{8}j_3)\cos\beta]$ . In Fig. 2, the overlap functions for the two representative pairs are shown.

Here, we give a simple interpretation for the angular dependence of Eqs. (7) and (8). The beam pattern functions  $F_a^P$  and  $F_b^P$  are given by linear combinations of  $(\cos(2\sigma_1), \sin(2\sigma_1))$  and  $(\cos(2\sigma_2), \sin(2\sigma_2))$ , respectively, reflecting their spin-2-like nature. Then, with Eq. (5) and addition formulas of trigonometric functions, the overlap functions should be linear combinations of  $\cos(4\Delta)$ ,  $\cos(4\delta)$ ,  $\sin(4\Delta)$ , and  $\sin(4\delta)$ . Since the expectation value  $C_{ab}(f)$  is a real function for our beam pattern functions, we have  $\langle s_a s_b^* \rangle = \langle s_b s_a^* \rangle$ . This essentially results in replacing the roles of  $\sigma_1$  and  $\sigma_2$ , and the functions  $\gamma_I$  and  $\gamma_V$  cannot contain terms proportional to  $\sin(4\delta) = \sin[2(\sigma_1 - \sigma_2)]$ .

On the other hand, while the observable  $C_{ab}(f)$  and the amplitude  $I$  are invariant under the parity transformation of a coordinate system, the sign of the parameter  $V$  flips. This is because the transformation interchanges right- and left-handed waves. Therefore, the function  $\gamma_{V,ab}$  must change its sign while keeping the quantity  $C_{ab}(f)$  invariant. Geometrically, this corresponds to the redefinition of the azimuthal angles  $\sigma_{1,2}$  in a clockwise direction (or putting  $\sigma_1 \rightarrow -\sigma_1$  and  $\sigma_2 \rightarrow -\sigma_2$ ). As a result, the function  $\gamma_{V,ab}$

TABLE I. Upper right ( $\beta, \cos(4\delta)$ ). Lower left ( $\cos(4\Delta), \sin(4\Delta)$ ).

	A	C	H	L	V
A: AIGO	*	70.8°, -0.61	135.6°, -0.82	157.3°, -0.88	121.4°, 0.23
C: LCGT	-0.58, 0.81	*	72.4°, 1.00	99.2°, -0.98	86.6°, -0.43
H: LIGO (Hanford)	-1.00, -0.007	-0.21, 0.98	*	27.2°, -1.00	79.6°, -0.43
L: LIGO (Livingston)	0.99, 0.15	0.04, -1.00	-0.36, -0.93	*	76.8°, -0.29
V: Virgo	-0.45, -0.89	0.92, 0.38	-0.76, -0.65	0.89, -0.46	*

should be odd functions of  $\delta$  and  $\Delta$ , and it must be proportional to  $\sin(4\Delta)$  as shown in Eq. (8) [with  $\sin(4\delta)$ -term being prohibited]. With similar arguments, we find that the function  $\gamma_I$  is a linear combination of  $\cos(4\Delta)$  and  $\cos(4\delta)$  as in Eq. (7).

The overlap function  $\gamma_{V,ab}$  always vanishes for a pair of detectors in the same plane ( $\beta = 0$ ), even with a finite separation  $D \neq 0$ . This cancellation comes from the geometric symmetry of the beam pattern function with respect to the plane [4,8].

*Broadband SNR.*—Now, we turn to focus on a broadband sensitivity to the  $I$  and  $V$  modes. In the weak signal limit, the total signal-to-noise ratio (SNR) for the correlation signal  $C_{ab}(f)$  is given by [5]

$$\text{SNR}^2 = \left( \frac{3H_0^2}{10\pi^2} \right)^2 T_{\text{obs}} \left[ 2 \int_0^\infty df \frac{X^2}{f^6 N_a(f) N_b(f)} \right], \quad (9)$$

with  $X = \gamma_I \Omega_{\text{GW}} + \gamma_V \Omega_{\text{GW}} \Pi$ . We denote the noise spectra for detectors  $a$  and  $b$  by  $N_a(f)$  and  $N_b(f)$ , assuming no noise correlation between them. In what follows, we fur-

ther assume that all the detectors have the same sensitivity comparable to the noise spectral curves of advanced LIGO. The analytical fit from Fig. 1 of Ref. [9] leads to  $N(f) = 10^{-44}(f/10 \text{ Hz})^{-4} + 10^{-47.25}(f/10^2 \text{ Hz})^{-1.7} \text{ Hz}^{-1}$  for  $10 \text{ Hz} \leq f \leq 240 \text{ Hz}$ ,  $N(f) = 10^{-46}(f/10^3 \text{ Hz})^3 \text{ Hz}^{-1}$  for  $240 \text{ Hz} \leq f \leq 3000 \text{ Hz}$ , and otherwise  $N(f) = \infty$ . The combination  $f^6 N(f)^2$  becomes minimum around  $f \sim 50 \text{ Hz}$  with its bandwidth  $\Delta f \sim 100 \text{ Hz}$ . For a pair of coincident detectors (i.e.,  $\gamma_{I,ab} = 1$  and  $\gamma_{V,ab} = 0$ ), we numerically obtain  $\text{SNR}_0 = 4.8(T_{\text{obs}}/3 \text{ yr})^{1/2} \times (\Omega_{\text{GW}} h_{70}^2 / 10^{-9})$  by setting  $X = \Omega_{\text{GW}}$  in Eq. (9).

The total SNR depends strongly on model parameters of the background, including the polarization degree  $\Pi$ . In order to present our numerical results concisely, we first calculate  $\text{SNR}_{\{I,V\},ab}$  by plugging  $X = \gamma_{\{I,V\},ab}$  into Eq. (9) and then normalize them as  $S_{\{I,V\},ab} \equiv \text{SNR}_{\{I,V\},ab} / \text{SNR}_0$ .

*Optimal configuration.*—Let us discuss optimal configurations of two detectors ( $a, b$ ) for measuring the  $I$  and  $V$  modes with the correlation signal  $C_{ab}$ . There are two relevant issues here: maximization of  $S_{I,ab}$  and  $S_{V,ab}$ , and switching off either of them ( $S_{I,ab} = 0$  or  $S_{V,ab} = 0$ ) for their decomposition. To deal with the situation comprehensively, we consider how to set the second detector  $b$  relative to the fixed first one  $a$  with a given separation angle  $\beta$ . In this case, there are two adjustable parameters,  $\sigma_1$  and  $\sigma_2$ . The former determines the position of the detector  $b$ , while the latter specifies its orientation (see Fig. 1). Based on the expressions (7) and (8), one finds that there are three possibilities for the optimal detector orientation:  $\cos(4\Delta) = -\cos(4\delta) = \pm 1$  (type I) or  $\cos(4\Delta) = \cos(4\delta) = \pm 1$  (type II) to maximize the normalized SNR  $S_{I,ab}$  [5], and  $\cos(4\Delta) = \cos(4\delta) = 0$  (type III) to erase the contribution from  $I$  mode. For type I, the solutions of the two angles  $\sigma_{1,2}$  are  $\sigma_1 = \sigma_2 = 45^\circ \pmod{90^\circ}$  and the detector  $b$  must be sited in one of the two great circles passing through the detector  $a$ , parallel to one of the two arms. For type II, the second detector must reside in two great circles parallel or perpendicular to the bisecting line of each detector. Similarly, the type III configuration is realized by placing the second detector on one of the four great circles defined for types I and II, with rotating  $45^\circ$  relative to the first detector.

Note that the sensitivity to the  $V$  mode is automatically switched off for the type I and II configurations and is conversely maximized for the type III configuration. This is because the normalized SNR  $S_{V,ab}$  is proportional to  $\sin(4\Delta)$ . In this sense, the condition for type III is geomet-

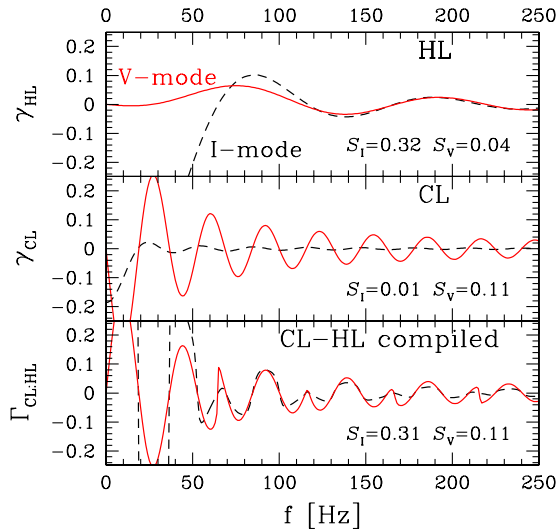


FIG. 2 (color online). Overlap functions for the unpolarized  $I$  mode (dashed curves), and the circularly polarized  $V$  mode (solid curves). The upper panel shows the results for the Hanford-Livingston (HL) pair (the characteristic frequency  $f_D = 100 \text{ Hz}$ ). The middle one is results for the LCGT-Livingston (CL) pair ( $f_D = 31 \text{ Hz}$ ). The normalized SNRs  $S_{I,V}$  (with the adv LIGO noise spectrum) are also presented. The bottom one show the compiled functions  $\Gamma_{I,V}$  [Eq. (10)] made from both pairs.

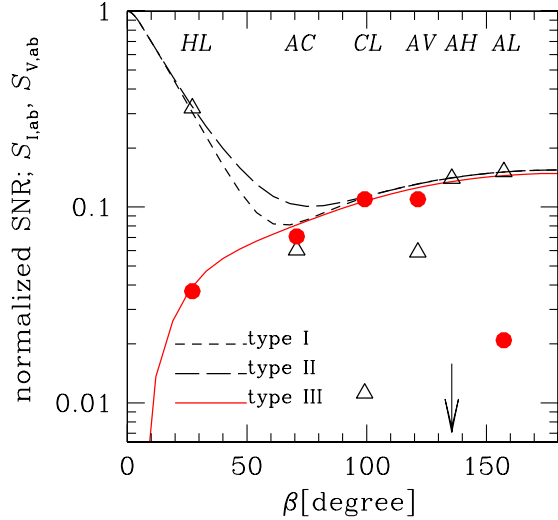


FIG. 3 (color online). Normalized signal-to-noise ratios ( $S_{I,ab}$  and  $S_{V,ab}$ ) with optimal configurations for the  $I$  mode (short dashed curve: type I, long dashed curve: type II) and for the  $V$  mode (solid curve: type III with setting  $\Pi = 1$  for illustrative purposes). We use the noise curve for the advanced LIGO. For each detector pair,  $S_I$  and  $S_V$  are given with a triangle and a circle, respectively, at its separation  $\beta$ . There are four other pairs not shown here: CH with  $(S_I, S_V) = (0.04, 0.08)$ , LV with  $(0.08, 0.04)$ , HV with  $(0.07, 0.06)$ , and CV with  $(0.09, 0.04)$ .

rically severe. For a nonoptimal pair of detectors, a definite detection of  $V$ -mode signal seems rather difficult due to the mixture of the  $I$ - and  $V$ -mode signals. As we see later, however, we can easily control the contribution from the  $I$  (or  $V$ ) mode by introducing a third detector.

In Fig. 3, we present the normalized SNRs for the optimal geometries: types I, II, and III. One noticeable point is that a widely separated ( $\beta \sim 180^\circ$ ) pair is powerful to search for the  $V$  mode (recall the cancellation  $\gamma_V = 0$  at  $\beta = 0$ ). To reduce the contribution from the  $I$  mode, pairs that are usually disadvantageous to measuring the total intensity  $\Omega_{\text{GW}}$  now play a very important role. In Fig. 3, we also show the normalized SNRs for representative pairs made from the five detectors, in which several interesting combinations are found. The Hanford-Livingston (HL) pair [with  $\cos(4\delta) \sim 1$  and  $\sin(4\Delta) \sim 0.93$ ] realizes nearly maximum values simultaneously for  $S_{I,ab}$  and  $S_{V,ab}$  at  $\beta = 27.2^\circ$ . This is because  $S_{I,ab}$  is mainly determined by the angle  $\delta$  at a small  $\beta$ , while  $S_{V,ab}$  depends only on  $\Delta$ . The LCGT-Livingston (CL) pair has good sensitivity to the  $V$  mode and is relatively insensitive to the  $I$  mode. In contrast, the AIGO-LIGO-Hanford (AH) pair is almost insensitive to the  $V$  mode. LCGT and AIGO detectors are suitably oriented to probe the  $I$  and  $V$  modes, respectively.

*Separating  $I$  and  $V$  modes.*—As a final mention, we will address the issue of  $I$  and  $V$  mode separation by combining several pairs of detectors. For preliminary investigation, we consider the case that two pairs of interferometers ( $a, b$ ) and ( $c, d$ ) are available. Detectors  $a$  and  $c$  can be identical, but we need at least three independent detectors for the

study below. First note that the correlation signals are given by  $C_{ab}(f) = \gamma_{I,ab}(f)I(f) + \gamma_{V,ab}(f)V(f)$  and  $C_{cd}(f) = \gamma_{I,cd}(f)I(f) + \gamma_{V,cd}(f)V(f)$ . From this, one can easily find that the contribution from the  $I$  mode is canceled by taking a combination  $W \equiv \gamma_{I,ab}C_{cd} - \gamma_{I,cd}C_{ab} = (\gamma_{V,cd}\gamma_{I,ab} - \gamma_{V,ab}\gamma_{I,cd})V(f)$ . The statistical analysis based on  $W$  would be a robust approach for  $V$ -mode search, although a further refinement may be possible by combining more pairs.

Since the rms amplitude of the detector noise for the combination  $W$  becomes  $N(f)(\gamma_{I,ab}^2 + \gamma_{I,cd}^2)^{1/2}$ , we define the *compiled* overlap function for the  $V$  mode by

$$\Gamma_{V,ab:cd} \equiv \frac{\gamma_{V,cd}\gamma_{I,ab} - \gamma_{V,ab}\gamma_{I,cd}}{[\gamma_{I,ab}^2 + \gamma_{I,cd}^2]^{1/2}}. \quad (10)$$

This expression should be used in Eq. (9) when evaluating the broadband SNR for the  $V$  mode with the combination  $W$ . In a similar way, we define the compiled function  $\Gamma_{I,ab:cd}$  for the  $I$  mode by interchanging the subscripts  $V$  and  $I$  in Eq. (10). The bottom panel of Fig. 2 shows the compiled overlap functions  $\Gamma_{\{I,V\},ab:cd}$  from two pairs; CL-HL. With this combination, the normalized SNR becomes 0.11 for the  $V$  mode and 0.31 for the  $I$  mode. Using numerical results below Eq. (9), the detection limit for the polarization degree  $\Pi$  is given as  $\Pi = (T/3 \text{ yr})^{-1/2} \times (\text{SNR}_V/5)(\Omega_{\text{GW}}h_{70}^2/10^{-8})^{-1}$  with signal-to-noise ratio  $\text{SNR}_V$ . These numerical results are almost the same values as in  $S_V$  for CL and  $S_I$  for HL, and the  $I$ -,  $V$ -mode separation can be performed efficiently with naively expected sensitivities  $S_{\{I,V\},ab}$ . The other combinations, such as AV-HL and CL-HV, also provide the normalized value  $\sim 0.11$  for the  $V$  mode, but AH-AL has only 0.015.

We would like to thank N. Kanda and M. Ando for helpful conversations. This work was supported in part by JSPS Grant No. 18740132.

- 
- [1] B. Abbott *et al.*, Phys. Rev. Lett. **95**, 221101 (2005).
  - [2] S.H.S. Alexander, M.E. Peskin, and M.M. Sheikh-Jabbari, Phys. Rev. Lett. **96**, 081301 (2006); M. Satoh *et al.*, arXiv:0706.3585.
  - [3] A. Lue, L. Wang, and M. Kamionkowski, Phys. Rev. Lett. **83**, 1506 (1999); C. Caprini, R. Durrer, and T. Kahniashvili, Phys. Rev. D **69**, 063006 (2004); S. Saito, K. Ichiki, and A. Taruya, arXiv:0705.3701.
  - [4] N. Seto, Phys. Rev. Lett. **97**, 151101 (2006); Phys. Rev. D **75**, 061302(R) (2007).
  - [5] E.E. Flanagan, Phys. Rev. D **48**, 2389 (1993).
  - [6] B. Allen and J.D. Romano, Phys. Rev. D **59**, 102001 (1999).
  - [7] N. Arnaud *et al.*, Phys. Rev. D **65**, 042004 (2002); K. Kuroda *et al.*, Int. J. Mod. Phys. D **8**, 557 (1999).
  - [8] H. Kudoh and A. Taruya, Phys. Rev. D **71**, 024025 (2005).
  - [9] E. Gustafson *et al.*, 1999, LIGO project document No. T990080-00-D.